JOURNAL OF MATERIALS PROCESSING TECHNOLOGY 209 (2009) 1861–1870

journal homepage: www.elsevier.com/locate/jmatprotec

Magnetorheological fluid-controlled boring bar for chatter suppression

Deqing Mei[a,*], *Tianrong Kong*[a], *Albert J. Shih*[b], *Zichen Chen*[a]

[a] *Department of Mechanical Engineering, Zhejiang University, Hangzhou 310027, PR China*
[b] *Department of Mechanical Engineering, University of Michigan, Ann Arbor, MI 48109, USA*

ARTICLE INFO

Article history:
Received 5 December 2007
Received in revised form
14 April 2008
Accepted 19 April 2008

Keywords:
Chatter suppression
MR fluid
Boring bar
Dynamic model
Stability

ABSTRACT

An innovative chatter suppression method based on a magnetorheological (MR) fluid-controlled boring bar for chatter suppression is developed. The MR fluid, which changes stiffness and undergoes a phase transformation when subjected to an external magnetic field, is applied to adjust the stiffness of the boring bar and suppress chatter. The stiffness and energy dissipation properties of the MR fluid-controlled boring bar can be adjusted by varying the strength of the applied magnetic field. A dynamic model of a MR fluid-controlled boring bar is established based on an Euler–Bernoulli beam model. The stability of the MR fluid-controlled boring system is analyzed, and the simulation results show that regenerative chatter can be suppressed effectively by adjusting the natural frequency of the system. Experiments in different spindle speeds utilizing a MR fluid-controlled boring bar are conducted. Under a 1 Hz square wave current, chatter can be suppressed, as evidenced by the elimination of chatter marks on the machined surfaces and the reduction in the vibration acceleration at the tip of the boring bar.

© 2008 Elsevier B.V. All rights reserved.

1. Introduction

The vibration of tools used in machining operations plays a key role in hindering the productivity of those processes. Excessive vibrations accelerate tool wear, cause poor surface finish, and may damage spindle bearings (Altintas, 2000). Chatter is a self-excited vibration phenomenon common in machining. In deep hole boring, the long, cantilevered boring bars have inherently low stiffness. This makes them prone to chatter, even at very small cutting depths. Chatter during the boring process directly influences the dimensional accuracy, surface quality, and material removal rate (Tlusty, 2000). Suppressing the chatter effectively in deep hole boring is important.

Research in boring chatter suppression has been conducted during the past several decades. Tewani et al. (1995) used an active dynamic absorber to suppress machine tool chatter in a boring bar, the vibrations of the system are reduced by moving an absorber mass using an active device such as an piezoelectric actuator. Tanaka and Obata (1994) suppressed the chatter of slender boring bar using piezoelectric actuators, chatter vibration signals detected by a pickup are fed to a computer. Marra et al. (1995) designed a H_∞ controller to eliminate the vibrations in cutting operations with a active piezoelectric actuators. Li et al. (2006) investigated the effects of varying spindle speed. Pratt and Nayfeh (2001) suppressed chatter with a magnetorestrictive actuator, and Pan et al. (1996) proposed actively controlling such an actuator. Wong et al. (1995) applied actively controlled electromagnetic dynamic absorbers. Li and Hu (1997) suppressed chatter by using a dynamic damper. Rivin and Kang (1992) described a systemic approach to the development of cantilever boring bar tooling structures. Finally, Wang and Fei (1999) developed

* *Corresponding author*. Tel.: +86 571 87951906.
E-mail addresses: medqmei@zju.edu.cn, medqmei@umich.edu (D. Mei).
0924-0136/$ – see front matter © 2008 Elsevier B.V. All rights reserved.
doi:10.1016/j.jmatprotec.2008.04.037

an on-line chatter detection and control system utilizing electrorheological (ER) fluid.

Based on the mode of chatter suppression employed, suppression methods can be classified into three types: passive, active, and semi-active. Passive chatter suppression is simple in structure, but the dynamic parameters of the damper used cannot be adjusted, leading to poor performance when the working condition changes. Li and Hu (1997) suppressed chatter by using a dynamic damper, and Rivin and Kang (1992) developed a cantilever boring bar tooling structures, belong to the passive chatter suppression method. Active chatter suppression allows for continuously adjustable dynamic parameters based on the feedback signals. The chatter suppression methods based on the effects of varying spindle speed (Li et al., 2006), piezoelectric actuator (Tewani et al., 1995), magnetorestrictive actuator (Pratt and Nayfeh, 2001) and actively controlled electromagnetic dynamic absorber (Wong et al., 1995) belong to active chatter suppression method. This type is more effective than passive methods, but it requires high power and is expensive. Finally, semi-active chatter suppression can improve stability by changing the inherent stiffness and dynamic damping parameters of a system (Wang and Fei, 1999). Semi-active chatter suppression not only has better damping effectiveness than the passive mode, but also has lower power and cost requirements than active suppression (Lam and Liao, 2001). A semi-active chatter suppression method employing the MR fluid is investigated in this study. MR fluid exhibits some advantages over typical ER materials. Compared to ER fluids (Wang and Fei, 1999), which have high working voltages (2–5 kV) and narrow working temperatures (10–70 °C), the power (1–2 A or 50 W) and voltage (12–24 V) requirements for MR fluid activation are relatively small, and the working temperatures (−40 to 150 °C) of MR fluid are relatively broadened. So MR fluids are more practical and suitable for machine tool applications. In addition, ER fluids are sensitive to impurities, which is not a problem for MR fluids (Srinivasan and McFarland, 2001).

In this study, a MR fluid-controlled chatter suppressing boring bar is proposed. The theory of chatter suppression using an MR fluid-controlled boring bar is first introduced. Next, the design and fabrication of a MR fluid-controlled boring bar is described. Finite element modeling (FEM) of the magnetic system is then detailed, the Euler–Bernoulli dynamic beam model of the MR fluid-controlled boring bar is created, and the stability of the MR fluid-controlled boring system is analyzed. Finally, a series of machining experiments in different spindle speeds to demonstrate chatter suppression based on MR fluid control of a boring bar are conducted for validation.

2. Theory of chatter suppression based on the MR fluid-controlled boring bar

Most chatter occurring in practical machining processes is what is termed regenerative chatter, which is usually caused by instability of the cutting process in combination with the mechanical structure of machining system. The frequency of regenerative chatter is close to the natural frequency of the machine tool (Merrit, 1965). The system dynamics of regenerative chatter is illustrated by the block diagram shown in

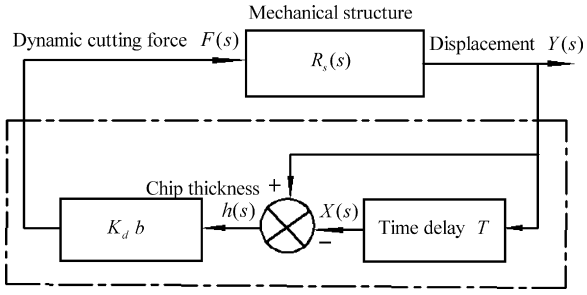

Fig. 1 – Block diagram of regenerative chatter dynamics (Yang and Tang, 1983).

Fig. 1 (Yang and Tang, 1983). The tool tip displacement $Y(s)$ is generated by the dynamic cutting force $F(s)$ applied at the tool tip. The dynamic behavior of the mechanical structures is expressed by the dynamic flexibility $R_s(s)$. The transient variation of chip thickness $h(s)$ is the difference between $Y(s)$ and the wavy surface $X(s)$ generated in the previous cutting pass. In an unstable cutting process, $F(s)$ will increase gradually. In boring, T is the period of spindle revolution, K_d is the cutting force coefficient (relating the cutting force to chip area), and b is the cutting width.

The mechanical structure of a boring system can be simplified to a single degree of freedom system modeled by a combination of equivalent mass (m), spring (k), and damping (c) elements (Altintas, 2000). The dynamic flexibility of the mechanical structure of the boring system can be expressed as follows (Yang and Tang, 1983):

$$R_s(\omega) = \frac{1}{(k - m\omega^2) + j c} \quad (1)$$

where ω is the frequency of vibration.

As shown in Fig. 2, $R_s(\omega)$ can be expressed in the complex plane as an arc, labeled I, with its center at (0, −1/2c) and a radius of 1/2c (Stephenson and Agapiou, 2006). The point (0, −1/c) is the intersection of arc I and the imaginary axis. At this

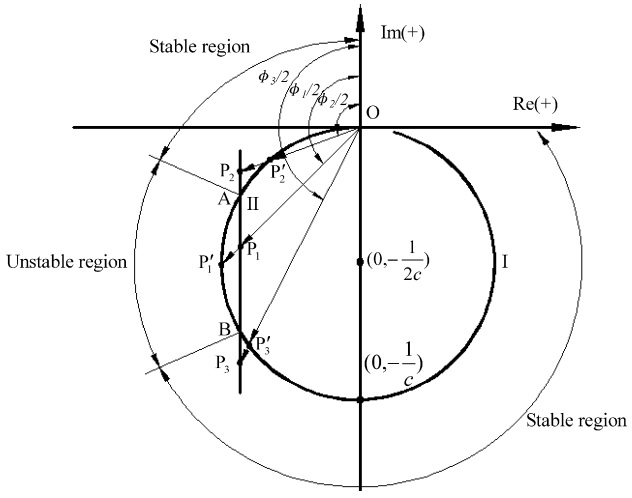

Fig. 2 – Dynamic flexibility curves of the mechanical structure and cutting process.

point, ω is equal to the natural frequency of the mechanical structure ω_n.

The dynamic behavior of the cutting process, including regeneration effects, can be described by the dynamic flexibility R_d (Yang and Tang, 1983):

$$R_d = \frac{1}{K_d b(\mu\ e^{-j\phi} - 1)} \quad (2)$$

where ϕ is the phase difference between the inner and outer modulations and μ is the overlap coefficient ($0 \le \mu \le 1$).

As shown in Fig. 2, R_d can be expressed in the complex plane as a line, marked II (with $\mu = 1$) (Stephenson and Agapiou, 2006). When the dynamic flexibility curves of the mechanical structure (I) and the cutting process (II) intersect, regenerative chatter will occur (Stephenson and Agapiou, 2006). As shown in Fig. 2, line II intersects arc I at points A and B, and divides arc I into stable and unstable regions.

The chatter frequency of the cutting process ω_c is (Yang and Tang, 1983):

$$\omega_c = \sqrt{\omega_n^2 + \frac{K_d b(1 - \cos\phi)}{m}} \quad (3)$$

where ω_n is the natural frequency of the mechanical structure of the boring system.

When chatter occurs, the vibration frequency ω is equal to ω_c, and the cutting process is located in the unstable region, as shown in Fig. 2. At this moment, if ω_n is changed by adjusting structural stiffness, ω will remain equal to ω_c for a short period of time. The cutting process will shift to the stable region because the vibration frequency is not equal to the resonant frequency of the system. Once in the stable region, the amplitude of vibration decays rapidly, and chatter is suppressed. However, the vibration frequency may shift to a new unstable resonant frequency during cutting, meaning the chatter could occur again.

If ω_n is changed continuously using MR fluid control, chatter can be suppressed. This concept is similar to changing spindle speed to suppress chatter (Li et al., 2006). When chatter occurs, the cutting process will be in the unstable region of arc I. At this moment, if ω_n can be increased by increasing the stiffness of the MR fluid-controlled boring bar, the dynamic flexibility of the mechanical structure $R_s(\omega)$ will be shifted in Fig. 2 from $\overrightarrow{OP_1}$ to $\overrightarrow{OP_2}$. According to Eq. (3), the chatter frequency ω_c will increase and shift to the stable region, because the phase difference ϕ_1 will remain the same for a short period. The dynamic flexibility of the cutting process R_d is shifted from $\overrightarrow{OP_1}$ to $\overrightarrow{OP_2}$. The cutting process is then in the stable region, and chatter is suppressed.

As the cutting process continues, it may again shift into the unstable region. When that happens, ω_n can be reduced by decreasing the stiffness of the MR fluid-controlled boring bar. Just as when ω_n is increased, $R_s(\omega)$ and R_d will be shifted to $\overrightarrow{OP_3}$ and $\overrightarrow{OP_3}$, respectively. The cutting process is then back within the stable region. Thus, conditions promoting regenerative chatter can be dealt with by either increasing or decreasing ω_n.

According to above theoretical analysis, as long as an innovative stiffness-tunable boring bar based on MR fluid can be developed, the chatter can be suppressed in boring process.

3. MR fluid and design and fabrication of a MR fluid-controlled boring bar

Magnetorheological materials are a class of material whose rheological properties may be rapidly varied by applying a magnetic field. Most commonly, these materials are fluids that consist of micron-sized, magnetically polarizable ferrous particles suspended in a carrier liquid. When exposed to a magnetic field, the suspended particles polarize and interact to form a structure aligned with the magnetic field that resists shear deformation or flow. This change in the material appears as a dramatic increase in apparent viscosity, or the fluid develops the characteristics of a semi-solid state. MR fluid rheological parameters (such as apparent viscosity and shearing stress) can be controlled by changing the intensity of magnetic field (Ginder et al., 1996). The main characteristics of MR effect are as follows: (1) *Reversibility*. The viscosity of MR fluid increases as the strength of the magnetic field increases, and even it can behave as semi-solid. When the applied magnetic field vanishes, the MR fluid reverts to its previous, more fluid state. The shift between liquid phase and

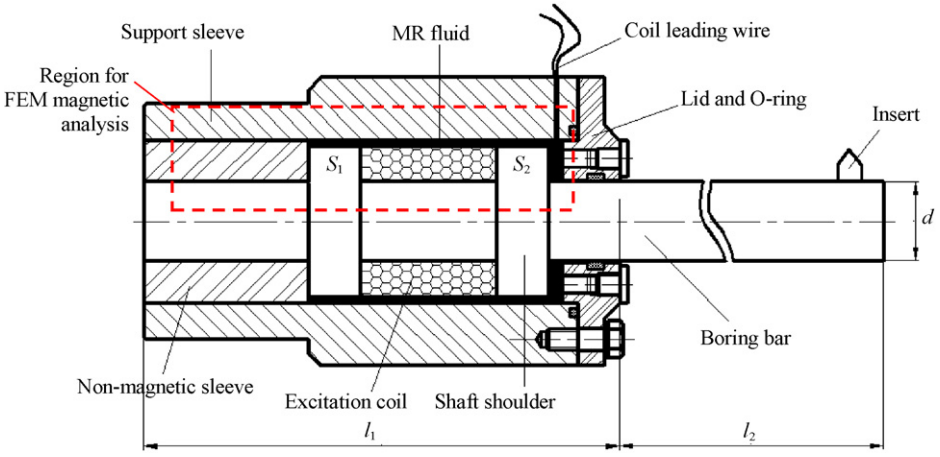

Fig. 3 – Structure of the MR fluid-controlled boring bar with chatter suppression.

solid phase is reversible. (2) *Controllability*. This change is in proportion to the magnitude of the magnetic field applied. In different intensities of magnetic field, the magnetic fluid shows different rheological characteristics, thus the MR equipment can be controlled by the utilization of magnetic field intensity signal. (3) *Quick-response*. In the applied magnetic field, the MR fluid has sensitive response. The transformation between the liquid and solid phases is fast, on the order of milliseconds (Schwartz, 2002). The response time of the MR fluid we used in this research is about 5–8 ms, so its corresponding bandwidth is about 125–200 Hz. For the innovative chatter suppression method proposed in this paper, we just need to input a 1–5 Hz periodical square wave current to MR fluid-controlled boring bar, so the response time of MR fluid is quick enough for the natural frequency adjustment and control in this research.

By surrounding the base of the boring bar with MR fluid, as shown in Fig. 3, the stiffness and natural frequency of the boring bar can be continuously varied by changing the intensity of the magnetic field passing through the MR fluid. The boring bar assembly in Fig. 3 consists of the MR fluid, a support sleeve, a non-magnetic sleeve, an excitation coil, and a boring bar shaft with two shoulders, marked as S_1 and S_2. To fabricate this boring bar assembly, the excitation coil is first embedded between the two shaft shoulders of the boring bar and coated with ethoxyline resin. The non-magnetic sleeve and support sleeve are then assembled. The MR fluid is poured into the annular cavity and then sealed in by a lid and O-rings. The thickness of the MR fluid layer in the annular cavity is about 1.0 mm. The diameter of the boring bar d is 30 mm, the ratio of length and diameter l_2/d is 6, and the length of the fixed portion l_1 is 200 mm.

4. FEM analysis of magnetic system for the MR fluid-controlled boring bar

The magnetic system for the MR fluid-controlled boring bar is important for energy transformation efficiency, as well as the chatter suppression capability of the system. FEM analysis was applied to analyze and design the magnetic field. The boring bar and support sleeve are made of AISI 1020 low-carbon steel with a magnetic conductivity of 1000 H/m. The non-magnetic sleeve and excitation coil are made of non-magnetic mallet alloy with a magnetic conductivity of only 1.5 H/m. The MR fluid is MRF-J01, produced by the Chongqing Instrument Material Research Institute in China. The magnetic conductivity of this MR fluid is 10 H/m.

An axisymmetric FEM model of the magnetic system was used to analyze the area, marked in Fig. 3, of the MR fluid-controlled boring bar. The finite element mesh consists of 545 nodes and 485 eight-node, quadrilateral elements, as shown in Fig. 4(a). For the boundary condition, the magnetic leakage across the boundary of the mesh is assumed to be zero.

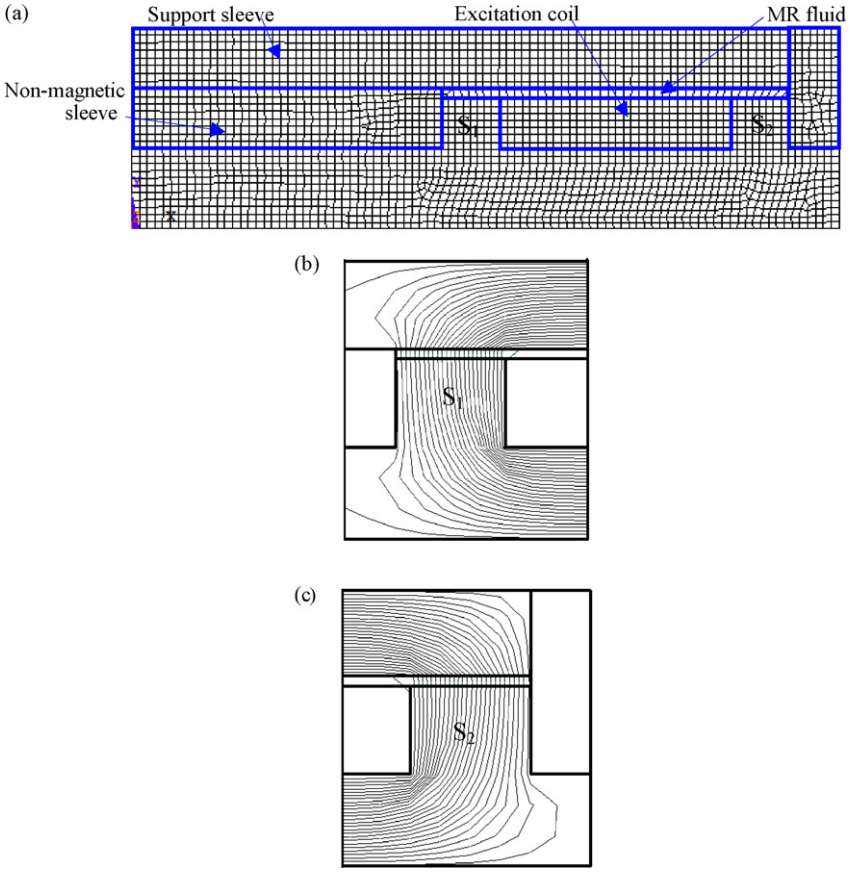

Fig. 4 – FEM model of, and results for, the magnetic system for a MR fluid-controlled boring bar. (a) The FEM mesh of the magnetic system of a MR fluid-controlled boring bar. (b) Distribution of the magnetic lines of flux in shaft shoulder S_1. (c) Distribution of the magnetic lines of flux in shaft shoulder S_2.

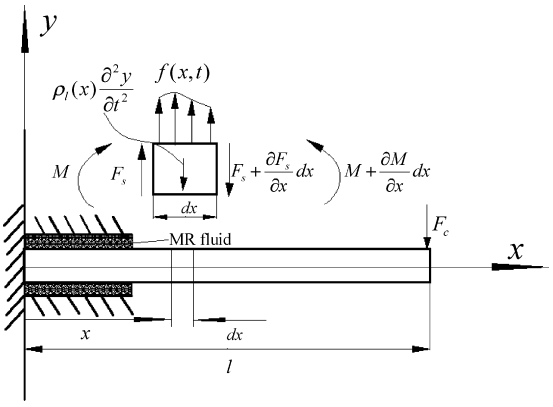

Fig. 5 – Dynamic model of a MR fluid-controlled boring bar.

The direction of magnetic flux is thus parallel to the boundary line. The current density of the excitation coil is calculated according to circuit theory and set as 267 A/cm^2.

Plots of the magnetic lines of flux in shaft shoulders S_1 and S_2 are shown in Fig. 4(b) and (c), respectively. The geometry of the boring bar components was designed with the goals that the magnetic lines of flux are perpendicular to the thin layer of MR fluid in shaft shoulders S_1 and S_2, and most magnetic lines of flux can go through two shoulders, thus enabling better actuation of the MR fluid. Fig. 4(b) and (c) shows that, at S_1 and S_2, the magnetic lines of flux are perpendicular to the thin layer of MR fluid, and most magnetic lines of flux are all going through shoulders S_1 and S_2. So the FEM analysis of magnetic system for the MR fluid-controlled boring bar shows that the design of its magnetic system is reasonable.

5. Dynamic modeling of the MR fluid-controlled boring bar

In this research, the ratio of length to diameter of the MR fluid-controlled boring bar is 6, the workpiece has a stiffness value much greater than that of the boring bar, so the bending mode of the boring bar need to be considered. Bending mode includes tangential vibrations and radial vibrations, tangential vibrations are in the direction of speed, so they will not affect regeneration of the chip load significantly but only the phase, but radial vibrations will change the depth of cut. Otherwise, axial stiffness and torsional stiffness of the boring bar are much greater than in bending, the boring bar is considered to be rigid in axial direction and torsional direction. So in our modeling process, the tangential vibrations, axial vibrations and torsional vibrations can be ignored, the boring bar can be modeled as a cantilevered beam in bending. An Euler–Bernoulli beam model of the MR fluid-controlled boring bar shaft shown in Fig. 5, and the equation describing the dynamics of the MR fluid-controlled boring bar can be expressed as (Wang et al., 2001):

$$\frac{\partial^2}{\partial x^2}\left[\mathrm{EI}(x)\frac{\partial^2 y(x,t)}{\partial x^2}\right]+\rho_l(x)\frac{\partial^2 y(x,t)}{\partial t^2}+C(x)\frac{\partial y(x,t)}{\partial t}=f(x,t) \quad (4)$$

where $\rho_l(x)$ is the mass of unit length of the boring bar, $\rho_l(x)=\rho S(x)$, $S(x)$ is the sectional area of the boring bar, ρ is the material density, $f(x,t)$ is the distributed load, $C(x)$ is the damping, $C(x)=C_s+\Delta C_m(x)$, $C_s(x)$ is the base viscous damping, and $\Delta C_m(x)$ is the variable damping generated by the MR fluid, $I(x)$ is the moment of inertia of the cross-sectional area, $E=E_s+\Delta E_m$ is the elastic modulus, E_s is the base elastic modulus, and ΔE_m is the variable elastic modulus generated by the MR fluid, $y(x,t)$ is the deflection of the boring bar.

Eq. (4) can be solved by using eigenfunction expansion of $y(x,t)$, yielding:

$$y(x,t)=\sum_{i=1}^{\infty}\phi_i(x)q_i(t) \quad (5)$$

where $\phi_i(x)$ and $q_i(t)$ ($i=1,2,3,\ldots,\infty$) are the mode and modal coordinates of the system, respectively. The boundary conditions at the fixed end ($x_0=0$) are $\phi(x_0)=0$ and $\phi'(x_0)=0$, and $\phi''(x_0)=0$ and $\phi'''(x_0)=0$ at the free end ($x_0=l$). The modes are mass-normalized as follows:

$$\int_0^l \rho_l(x)\phi_i(x)\phi_j(x)\,dx=\delta_{ij} \quad (i,j=1,2,3,\ldots) \quad (6)$$

$$\int_0^l \mathrm{EI}(x)\phi_i''(x)\phi_j''(x)\,dx=\omega_{ni}^2\delta_{ij} \quad (i,j=1,2,3,\ldots) \quad (7)$$

where l is the length of the boring bar, δ is Dirac delta function, and ω_{ni} is the ith natural frequency.

Eq. (4) can be rewritten in terms of the modal coordinates as follows:

$$\ddot{q}_i(t)+2\xi_i\omega_{ni}\dot{q}_i(t)+\omega_{ni}^2 q_i(t) = f_i(t)=\int_0^l f(x,t)\phi_i(x)\,dx \quad (i,j=1,2,3,\ldots) \quad (8)$$

where ξ_i, a number between 0 and 1, is the ith modal damping ratio and $f_i(t)$ is the generalized force corresponding to $q_i(t)$.

By considering the dynamic interaction between the cutting force and workpiece surface undulations (produced by

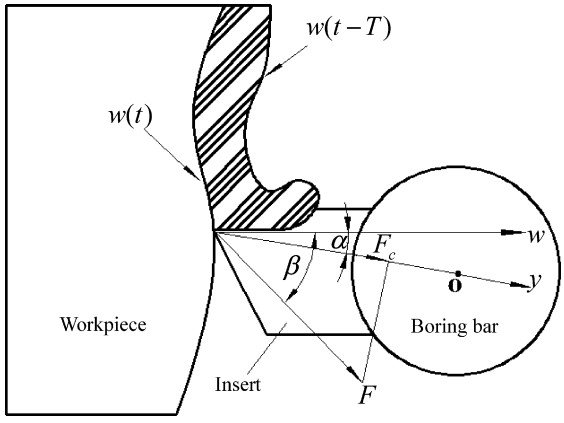

Fig. 6 – The cutting force model of a boring process.

previous revolutions during the cutting process), Eq. (4) can be changed to

$$\frac{\partial^2}{\partial x^2}\left[EI(x)\frac{\partial^2 y(x,t)}{\partial x^2}\right] + \rho_l(x)\frac{\partial^2 y(x,t)}{\partial t^2} + C(x)\frac{\partial y(x,t)}{\partial t} + F_c = 0 \quad (9)$$

where F_c is the cutting force, as illustrated in Fig. 6.

In Fig. 6, $w(t)$ is the inner modulation and $w(t-T)$ is the outer modulation. Considering the critical state of system stability, let $w(t) = A\cos wt$, where A is the amplitude of vibration at the tool tip. The cutting depth $\Delta s(t)$ can be expressed as

$$\Delta s(t) = w(t) - \mu w(t-T) = (1-\mu\ \cos\omega T)w(t) + \frac{\mu\sin\omega T}{\omega}\dot{w}(t) \quad (10)$$

If the cutting force is assumed to be proportional to the cross-sectional area of the cut, the dynamic cutting force F can be expressed as equal to $K_d b\Delta s(t)$, where K_d is the cutting stiffness. Let $w(t) = y(t)\cos\alpha$, the cutting force F_c can be expressed as

$$F_c = F\cos(\beta-\alpha) = K_d b\cos(\beta-\alpha) \times \cos\alpha\left((1-\mu\cos\omega T)y(t) + \frac{\mu\sin\omega T}{\omega}\dot{y}(t)\right) \quad (11)$$

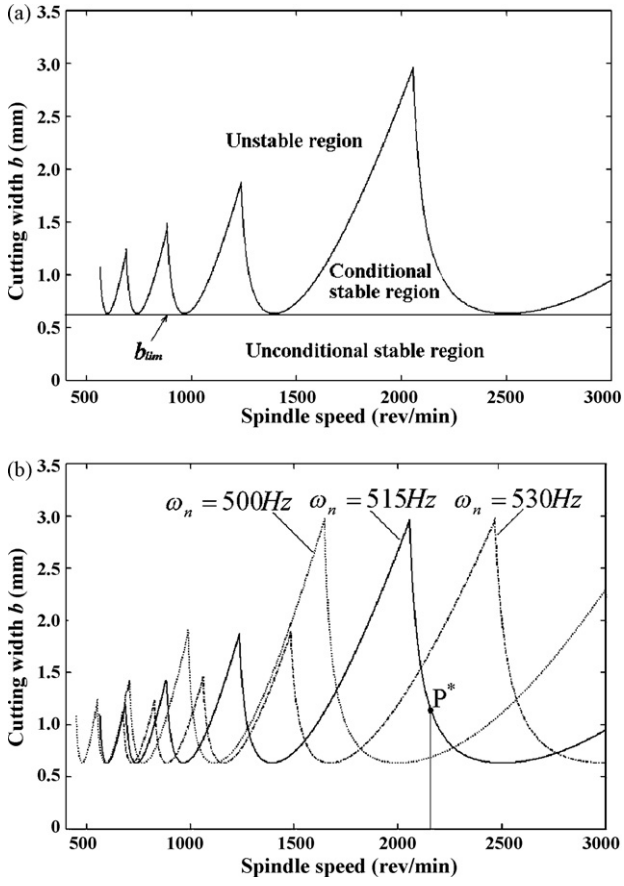

Fig. 7 – Stability lobe diagrams of the MR fluid-controlled boring process. (a) Stability lobe diagram of the original state. (b) Stability lobe diagram for varying ω_n.

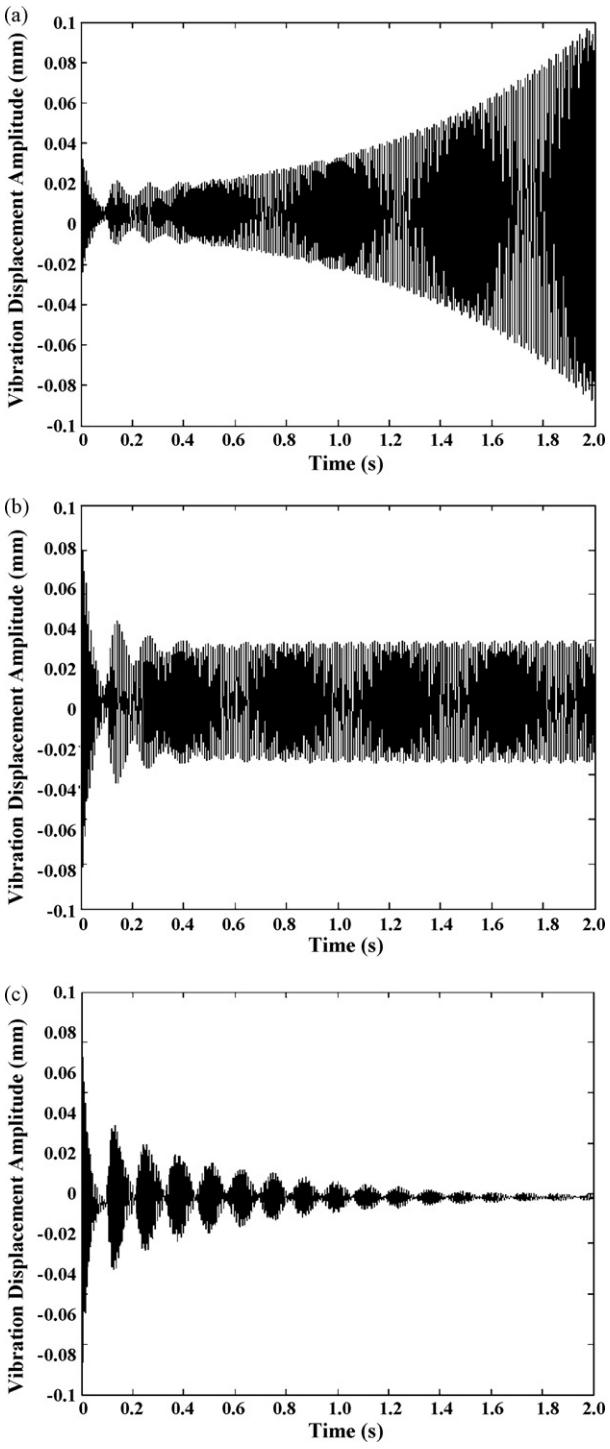

Fig. 8 – Vibration displacement of the boring bar at point P* with varying ω_n: (a) ω_n = 500 Hz, (b) ω_n = 515 Hz and (c) ω_n = 530 Hz.

where α is the angle between y and w, and β is the angle between F and w.

Substituting Eq. (11) into (9), and following the same derivation process used to convert Eq. (4) to (8), the corresponding dynamics equation, in terms of the modal coordinates, can be derived:

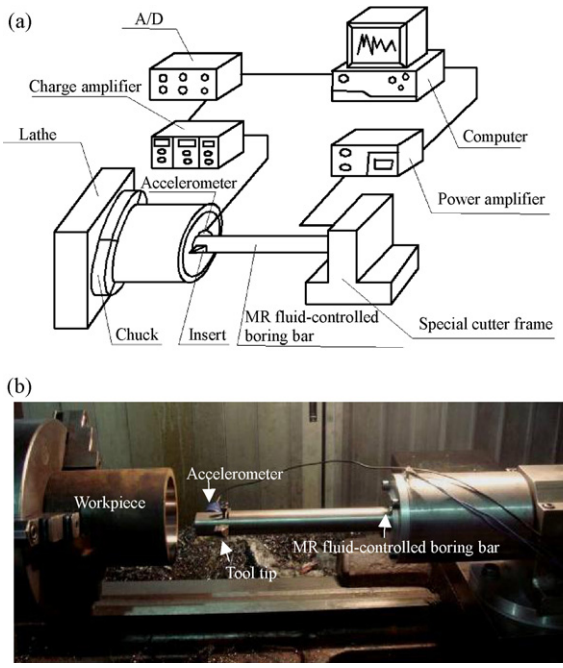

Fig. 9 – Experimental setup used to study a MR fluid-controlled boring bar. (a) Schematic of the experimental setup. (b) Photograph of the experimental setup on the lathe.

$$\ddot{q}_i(t) + \left(2\xi_i\omega_{ni} + \frac{O_i\mu\ \sin\omega T}{\omega}\right)\dot{q}_i(t) + (\omega_{ni}^2 + O_i(1-\mu\ \cos\omega T))q_i(t) = 0 \quad (12)$$

where $O_i = (\omega_{ni}^2 K_d b\cos(\beta-\alpha)\cos\alpha)/EI$.

Eq. (12) can be rewritten in matrix form as

$$M\ddot{Q}(t) + C\dot{Q}(t) + KQ(t) = 0 \quad (13)$$

where $M = I$, $Q(t) = [q_1(t),\ q_2(t), \ldots, q_n(t)]^T$, $C_{i,j} = \mathrm{diag}[2\xi_i\omega_{ni} + (O_i\mu\sin(\omega T))/\omega]$, and $K_{ij} = \mathrm{diag}[\omega_{ni}^2 + O_i(1-\mu\cos\omega T)]$ (i, j = 1, 2, 3, . . ., n).

6. Stability analysis and simulation of the MR fluid-controlled boring bar

Previous studies showed that usually only one dominating mode exists in the chatter exhibited by most machining processes (Yang and Tang, 1983). By assuming $n = 1$ and multiplying $m = \rho_l l$ to Eq. (13):

$$m\ddot{q}(t) + \left(C_s + \Delta C_m + \frac{ubK_d\mu\sin\omega T}{\omega}\right)\dot{q}(t) + [K_s + \Delta K_m + ubK_d(1-\mu\ \cos\omega T)]q(t) = 0 \quad (14)$$

where $u = \cos(\beta-\alpha)\cos\gamma^4$, $\gamma^4 = \rho_l\omega_{n1}^2/EI$, K_s is base stiffness, and ΔK_m is the variable stiffness generated by the MR fluid.

The system in Eq. (14) consists of three parts: (i) the stiffness and damping inherent in the system, (ii) the equivalent

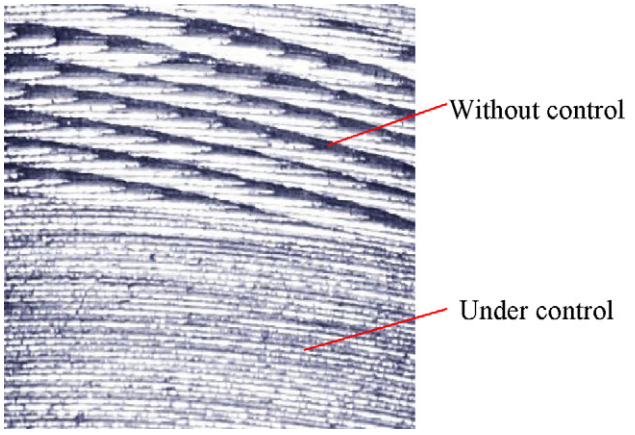

Fig. 10 – Picture of the machined surface after boring without and with MR fluid control (spindle speed = 200 rpm).

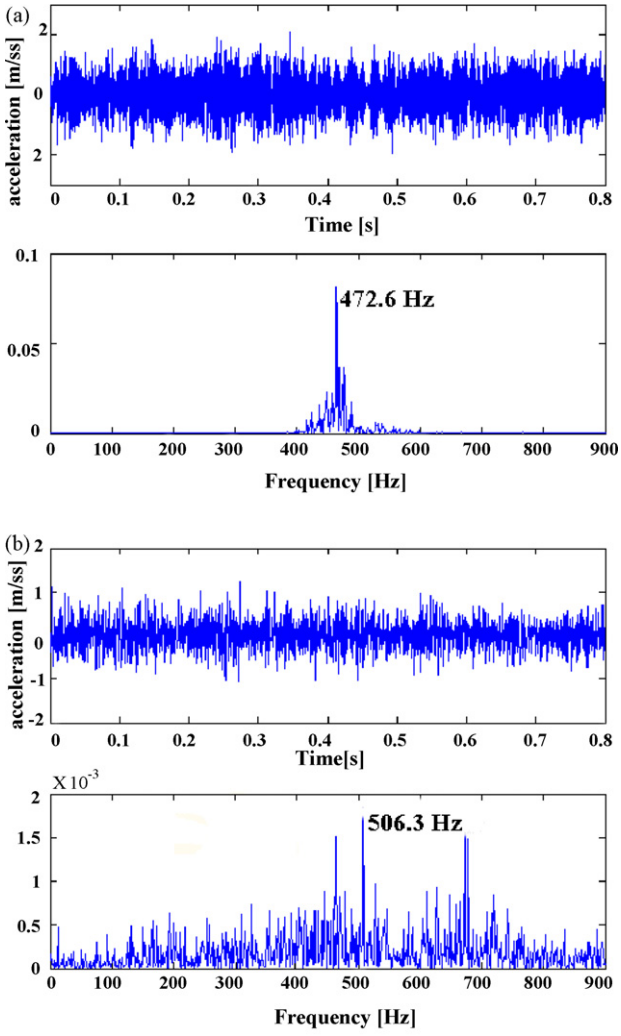

Fig. 11 – Vibration acceleration signal of the boring bar (spindle speed = 200 rpm). (a) Without MR fluid control. (b) With MR fluid control.

stiffness and damping produced by regenerative effects of the cutting process, and (iii) the equivalent variable stiffness and damping generated by the MR effect. Self-excited vibration occurs when the system damping of the boring process becomes negative. Thus, the critically stable state for the MR fluid-controlled boring system can be expressed as

$$C_s + \Delta C_m + \frac{ubK_d\mu \sin \omega T}{\omega} = 0 \quad (15)$$

Substituting Eq. (15) into (14), the result can be simplified to

$$m\ddot{q}(t) + [K_s + \Delta K_m + ubK_d(1 - \mu \cos \omega T)]q(t) = 0 \quad (16)$$

According to Eq. (16), the natural frequency of the cutting process ω_d in the critically stable state can be found to be

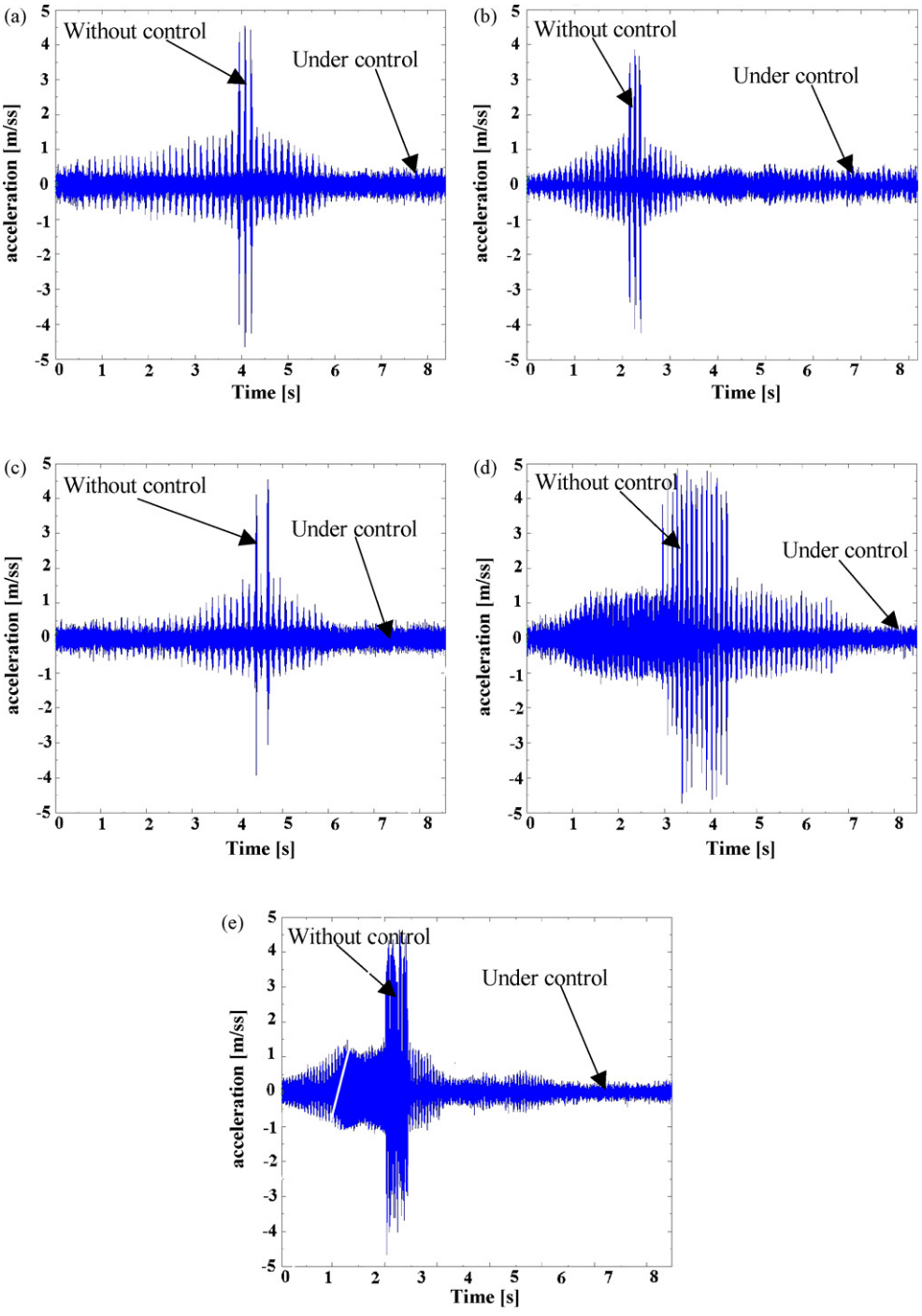

Fig. 12 – Time-domain vibration acceleration signal of the boring bar in different spindle speeds: (a) 450 rpm, (b) 560 rpm, (c) 710 rpm, (d) 900 rpm and (e) 1120 rpm.

$$\omega_d = \sqrt{\frac{K_s + \Delta K_m + ubK_d(1 - \mu \cos \omega T)}{m}} \quad (17)$$

As an example, let $K = K_s + \Delta K_m = 3200$ N/mm, $K_d = 1000$ N/mm^2, $\xi = (C_s + \Delta C_m)/(2m\omega_n) = 0.05$, $\omega_n = \sqrt{(1-\xi^2)K/m} = 2\pi \times 500$ rad/s, $\mu = 0.85$, and $u = 0.6$ (the parameters are evaluated from real machining process). Based on Eq. (17), the stability lobes, which represent the stability boundary, can be calculated. The results are shown in Fig. 7(a). The straight line at the bottom of lobes is the cutting width limit b_{lim}. Above the lobes is the unstable region. Between the lobes and the cutting width limit line is the conditional stable region. Below the cutting width limit line is the unconditional stable region.

When the stiffness of the MR fluid-controlled boring bar is adjusted, the system stability condition also changes. To study the effect of varying stiffness, the stability lobes for ω_n equals to 500, 515 and 530 Hz are shown in Fig. 7(b). The system stability lobes shift to the right, producing a broadened conditional stable region, as the natural frequency increases.

As an example to demonstrate boring chatter suppression, consider point P* in Fig. 7(b), with 2200 rev/min spindle speed and 1.2 mm cutting width. At $\omega_n = 500$ Hz, P* is in the unstable region and tool tip vibration amplitude is shown in Fig. 8(a). The vibration is amplified without limit, indicating chatter in the cutting process. When ω_n is increased to 515 Hz, P* is located on the stability lobes. The tool tip vibration amplitude, as shown in Fig. 8(b), is maintained at a constant level, which indicates the system is in the critical stable state. At $\omega_n = 530$ Hz, P* is in the conditional stable region and the amplitude of vibration of the tool tip, as shown in Fig. 8(c), decays quickly, thus making the cutting process stable.

These simulation results show that boring chatter can be suppressed by adjusting the natural frequency of the MR fluid-controlled boring bar.

7. Experimental validation

Experiments were carried out on a lathe. A schematic diagram and photograph of the experimental setup are shown in Fig. 9(a) and (b), respectively. The horizontal vibration of the tool tip was measured by a piezoelectric accelerometer placed at the free end of the boring bar. A computer, connected to a power amplifier, controls the current of the MR fluid-controlled boring bar. When chatter is detected, as measured by the behavior of the output signal produced by the accelerometer, the control system adjusts the waveform, frequency, and amplitude of the current applied on the coil. In this study, a square wave current with a frequency of 1 Hz and amplitude of 0–2 A was applied to the coil to generate the magnetic field for MR fluid control. The lathe spindle speed was set to 200 rpm, the feed rate was 0.1 mm/rev, and the cutting width was 0.2 mm. The workpiece was AISI 1020 low-carbon steel with an external diameter of 120 mm, an inner diameter of 100 mm, and a suspended length of 80 mm.

Fig. 10 shows a micrograph of the machined surface with and without MR control. Not only did the chatter marks disappear, but the surface roughness also decreased from 5 to 1 μm R_a when MR control was activated.

Fig. 11(a) shows the acceleration signal, in both the time and frequency domains, of the MR fluid-controlled boring bar without control when spindle speed is 200 rpm. The maximum vibration acceleration amplitude is about 2 m/s^2, and the main component of the chatter frequency is 473 Hz. When the square wave current is applied when spindle speed is 200 rpm, as shown in Fig. 11(b), the acceleration decreases to 1 m/s^2 in the time domain. In the frequency domain, the vibration frequency is evenly distributed without a dominating peak. And the values of accelerations in the frequency domain are about 50 times lower than in Fig. 11(a).

In order to investigate the effectiveness of the method in different spindle speeds, the spindle speed was changed to 450, 560, 710, 900 and 1120 rpm, some other chatter suppression experiments with MR fluid-controlled boring bar also have been conducted, and the results are shown in Fig. 12. The experimental results in different spindle speeds show that time-domain vibration acceleration signal of the boring bar decreased significantly when MR control was activated, and the chatter can be suppressed effectively after MR control.

These experimental results provide a clear demonstration of the effectiveness of chatter suppression using a MR fluid-controlled boring bar.

8. Conclusions

A chatter suppression method based on a MR fluid-controlled boring bar was presented and validated experimentally. The magnetic system inside the boring bar was designed using the FEM analysis. A dynamic Euler–Bernoulli beam model of the MR fluid-controlled boring bar was derived to analyze the regions of operating stability, and was also used to show that chatter could be suppressed by adjusting the damping and natural frequency of the system. Experimental results in different spindle speeds validated the model and demonstrated chatter suppression in a boring process.

A MR fluid-controlled tool can be applied to other machining processes for chatter suppression and material removal rate enhancement. Before this can happen, however, a more complicated dynamic model needs to be developed to enable more accurate simulation, and thus more effective design, of the next generation of MR fluid-based tool chatter suppression systems. Otherwise, according to Fig. 7(a), when the rotational speeds are slow, the chatter system will be in the left side of the stability diagram in this case, it is much easier to suppress the chatter by adjusting the natural frequency, and the simulation and experiment results have validated this. But when the rotational speeds are much higher, i.e. the chatter system will in the left side of the stability diagram, for such a case moving the chatter system into a lobe requires much higher increase in the stiffness, maybe increased damping effect is more useful in this case, and this needs to be investigated in the future.

Acknowledgements

The authors would like to acknowledge the supports from National Natural Science Foundation of China (grant nos. 50405036, 50775203), Hi-tech Research and Development Pro-

gram of China (grant no. 2006AA04Z329) and Natural Science Foundation of Zhejiang Province (grant no. Y104462).

REFERENCES

Altintas, Y., 2000. Manufacturing Automation: Metal Cutting Mechanics, Machine Tool Vibrations, and CNC Design. Cambridge University Press, Cambridge, UK.

Ginder, J.M., Davis, L.C., Elie, L.D., 1996. Rheology of magnetorheological fluids: models and measurements. International Journal of Modern Physics B 10, 3293–3303.

Lam, H.F., Liao, W.H., 2001. Semi-active control of automotive suspension systems with magnetorheological dampers. Proceedings of SPIE 4327, 125–136.

Li, C.J., Ulsoy, A.G., Endres, W.J., 2006. The effect of spindle speed variation on chatter suppression is rotating-tool machining. Materials Science Forum 505–507, 859–864.

Li, Q.T., Hu, R.S., 1997. The application of dynamic vibration absorbers in boring bars. Tool Technology 31 (11), 19–21 (in Chinese).

Marra, M.A., Walcott, B.L., Rouch, K.E., Tewani, S.G., 1995. H_∞ vibration control for machining using active dynamic absorber technology. In: Proceedings of the American Control Conference, Seattle, Washington, pp. 739–743.

Merrit, H.E., 1965. Theory of self-excited machine-tool chatter. ASME Journal of Engineering Industry 87, 447–454.

Pan, G., Xu, H., Kwan, C.M., Liang, C., Haynes, L., Geng, Z., 1996. Modeling and intelligent chatter control strategies for a lathe machine. In: Proceedings of the 1996 IEEE International Conference on Control Applications, Dearborn, MI, pp. 235–239.

Pratt, J.R., Nayfeh, A.H., 2001. Chatter control and stability analysis of a cantilever boring bar under regenerative cutting conditions. Philosophical Transactions: Mathematical, Physical and Engineering Science, Nonlinear Dynamics in Metal Cutting 359, 759–792.

Rivin, E.I., Kang, H., 1992. Enhancement of dynamic stability of cantilever tooling structures. International Journal of Machine Tools and Manufacture 32 (4), 539–561.

Schwartz, M., 2002. Encyclopedia of Smart Materials, vols. 1–2. John Wiley & Sons, New York.

Srinivasan, A.V., McFarland, D.M., 2001. Smart Structures: Analysis and Design. Cambridge University Press, Cambridge.

Stephenson, D.A., Agapiou, J.S., 2006. Metal Cutting Theory and Practice, second ed. CRC Press, Baca Raton.

Tanaka, H., Obata, F., 1994. Active chatter suppression of slender boring bar using piezoelectric actuators. JSME International Journal Series C—Dynamics Control Robotics Design and Manufacturing 37 (3), 601–606.

Tewani, S.G., Rouch, K.E., Walcatt, B.L., 1995. A study of cutting process stability of a boring bar with active dynamic absorber. International Journal of Machine Tools and Manufacture 35, 91–108.

Tlusty, J., 2000. Manufacturing Process and Equipment. Prentice Hall, Englewood Cliffs, NJ.

Wang, M., Fei, R.Y., 1999. Chatter suppression based on nonlinear vibration characteristic of electrorheological fluids. International Journal of Machine Tools and Manufacture 39, 1925–1934.

Wang, X.Q., So, R.M.C., Liu, Y., 2001. Flow-induced vibration of an Euler–Bernoulli beam. Journal of Sound and Vibration 243, 241–268.

Wong, B.W., Walcott, B.L., Rouch, K.E., 1995. Active vibration control via electromagnetic dynamic absorbers. In: Proceedings of the Fourth IEEE International Conference on Control Applications, Albany, NY, pp. 868–874.

Yang, S., Tang, H.L., 1983. Machine Tool Dynamics. China Machine Press, Beijing (in Chinese).